

TECHNOLOGIES FOR RELIABLE POWER DISTRIBUTION NETWORKS IN SAR EARTH OBSERVATION AND MULTIMEDIA COMMUNICATION SATELLITES

Reinhard Kulke, Dietmar Köther, Peter Uhlig Jürgen Kassner, Andreas Lauer, Matthias Rittweger

IMST GmbH, Carl-Friedrich-Gauss-Str.2, D-47475 Kamp-Lintfort, Germany
Tel. +49-2842-981-400, Fax +49-2842-981-499, kulke@imst.de

ABSTRACT

The use of active phased antenna arrays always requires power distribution networks as a part of Beam Forming Networks (BFN). In this area IMST has developed demanding technologies for three different missions in satellite SAR earth observation and multimedia communication. The basic idea behind the three concepts is the use of binary power distribution trees utilizing Wilkinson divider/combiner modules. The networks differ in particular in the application frequencies, the substrate technology as well as housing technique. They are characterized by excellent amplitude and phase balance, port-to-port isolation as well as thermal stability. All networks utilize standard materials in reliable manufacturing processes. The high frequency properties of the components (transitions, divider/combiner, shielding/radiation, matching...) have been developed and optimised by using accurate 3D field simulation based upon Finite Difference Time Domain (FDTD) method.

1. INTRODUCTION

In three projects different power divider / combiner networks have been designed, manufactured and characterised in X-, and L- and Ka-band. The following list summarizes the projects and the main properties of the networks:

- TerraSAR-X (LEO, Earth Observation): Flight Modules for EADS-Astrium and DLR/BMBF (Germany)
 - Power Divider @ 9.65 GHz (X-Band)
 - 1 : 32 Divider Network: 70 cm x 7.2 cm
 - Single-Layer PTFE Board (RT6002)
 - Aluminium housing includes shielding channels and SMA connector interfaces
- TerraSAR-L (LEO, Earth Observation) Pre-Development for EADS-Astrium (GB) and ESA-ESTEC
 - Power Divider @ 1.26 GHz (L-Band)
 - 3 x (1 : 7) Divider Networks: 120 cm x 20 cm
 - Multi-Layer PTFE Board (RT6002)
 - CFRP laminates for thermal and mechanical stability
 - SMA and GPO connector interfaces

- EASTON (Multimedia, Communication) Demonstrator for German Space Agency (DLR)
 - Power Divider @ 19 GHz (Ka-Band, Down-Link)
 - 2 x (1 : 4) Divider Networks: 6.5 cm x 3.5 cm
 - Multi-Layer LTCC Substrate (DuPont 951) with buried screen printed resistors
 - Gold plated DISPAL Housing with GPO interfaces

2. TERRA-SAR-X

For use in high-resolution X-band SAR satellite accurate (in terms of amplitude and phase) RF power distribution and combination is required to achieve optimum beam forming. Inaccuracies would influence beam shaping and thus degrade the performance of the earth observation satellite.

A planar power distribution network was developed to replace the waveguide arrangement used in previous missions. Among various planar power divider concepts the Wilkinson power divider / combiner was selected for its superior isolation in combination with good symmetry in amplitude and phase [0.1]. The complexity of a binary (1:32) divider and the requirement to distribute the signal also laterally led to a housing, which is large in terms of wavelength. Waveguide modes will allow signals to propagate not only along the designed transmission lines but also in any direction within the housing thus causing unwanted cross-talk and resonance. These effects degrade amplitude and phase performance. These waveguide modes can be avoided by either absorbing them with suitable material in the housing or by reducing the effective cross-section of the interior housing (operation below cut-off frequency for the waveguide mode).

2.1 Requirements

The spatial arrangement of the TR-modules defines the dimensions of the module: 700 mm x 72 mm x 8 mm. Compared to the wavelength $\lambda = 19.7$ mm @ 9.65 GHz, the housing is oversized. Cavity resonances can and will be excited at all discontinuities. If one or more of the cavity modes is excited, the influences of this mode on

amplitude and, even more critical, phase balance cannot be predicted or compensated. There are two approaches to suppress or prevent those unwanted modes:

- Suppression by absorption,
- Prevention by subdividing the housing in channels.

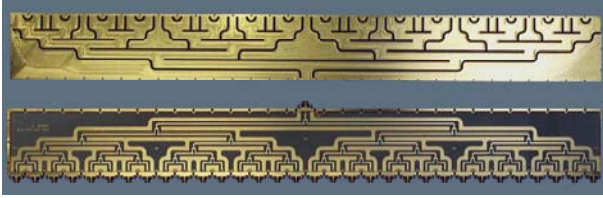


Fig. 1. Photograph of the 1:32 divider: housing, substrate and top cover

The first approach has the advantage of a fairly simple housing but it absorbs unwanted modes rather than avoiding them. A prototype has proven the effectiveness of the concept and its good-natured behaviour but the losses are about 3 dB higher than with the second method. In space, power consumption is an issue. Consequently a housing with channels has been preferred and realised. Substrate, housing and top cover of the final divider is shown in figure 1.

2.2 Subdividing the housing in channels

The classic method would be to mill grooves into the housing and insert the substrate, which is contoured to fit in this shape. Handling the delicate structure of this binary tree from contour milling to assembly would complicate the manufacturing process enormously. The concept presented here leaves the substrate in one rectangle and represents the channels with via chains (“fences”) in the substrate and grooves in the lid. Conductive elastomer gaskets provide electrical contact between substrate and lid. This technique becomes obvious in the photo of figure 2 and the cross-view schematic of figure 3.

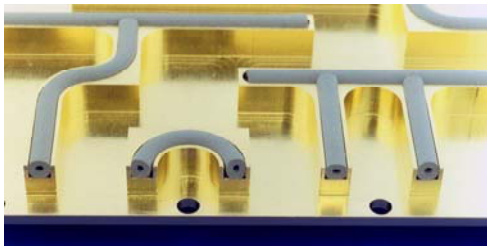


Fig. 2. Photo of the cover with grooves and gaskets

These walls subdivide the housing in channels whose cut-off frequency is well above 9.65 GHz. Conductive elastomer gaskets compensate for thermal mismatch of the materials involved and for the inevitable mechanical tolerances. After optimising the microstrip line in the channel for impedance, two microstrip lines in adjacent

channels separated by a wall with a conductive elastomer gasket were simulated with IMST’s 3D field simulator EMPIRE™ to verify the effectiveness of the shielding. A triple via chain resulted in 120 dB decoupling between the lines and was considered to have sufficient safety margin. The next step was to optimise the Wilkinson divider by simulating the complete structure taking into account not only the PCB-layout but also the real chip resistor with all parasitics and the influence of housing and lid.

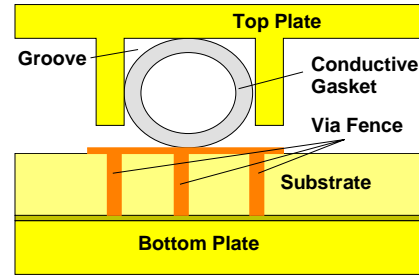


Fig. 3. Schematic of assembled "wall"

2.3 1:32 Divider

Based on these simulations and the results of some test structures, the complete 1:32 divider was designed, manufactured and tested. Insertion loss and amplitude balance turned out to be well within the ambitious specifications. See table 1 for a summary of parameters.

Table 1. Characteristics of X-band divider network

X-Band SAR Power Divider Network	
Centre Frequency	9.65 GHz
Band Width	200 MHz
Losses	≤ 2.9 dB
Amplitude Balance	± 0.26 dB
Phase Balance	$\pm 14.7^\circ$
Output Port Isolation	≥ 28.9 dB
Return Loss: Input Port 0	≥ 19.4 dB
Return Loss: Output Ports 1-32	≥ 21.8 dB

All 32 transmission paths showed very smooth phase vs. frequency, but the phase balance i.e. the phase difference between these 32 paths failed to fulfil specifications. The structure is designed to be absolutely symmetric; geometrical line lengths are diligently kept equal. Nevertheless, there is a phase imbalance of about $\pm 17^\circ$. A closer look at the substrate specification reveals a very likely cause for this difference in electrical length. The dielectric constant of this Rogers’ material is specified to be in the range of $\epsilon_r = 2.92 \pm 0.04$ [0.2]. Due to the large size, this tolerance can occur across one single circuit board. For the transmit path this translates into a phase variation of $\Delta\phi = \pm 40^\circ$! This worst case scenario assumes two paths with extreme values for the dielectric constant over the complete length, which is extremely unlikely but it explains the measured devia-

tion. The authors have published detailed simulated and measured results of the network development over the years within the papers [1.1] to [1.5].

3. TERRA-SAR-L

For L-band (1.3 GHz) SAR earth observation satellites an Elevation Feed Network (EFN) has been developed by the authors. The module consists of two receive (one for horizontal and one for vertical polarization as power combiner (RxH and RxV) and one transmit network as power divider (Tx). Since a binary tree is utilized, one port has to be terminated to achieve a (1:7) divider or combiner. The authors have designed a stack of 3 networks on top of each other within a multilayer PTFE laminate. Each network consists of 7 Wilkinson couplers which are connected with stripline waveguides. The advantages of this configuration are:

- One network realized on one substrate layer: a minimum number of transitions ensures excellent stability and balance behaviour,
- Wilkinson couplers show best divider/combiner properties also in cases of asymmetry within the network or a fault of a Tx/Rx module,
- high shielding and isolation can be achieved by using shielded stripline waveguides,
- additional CFRP panels ensure a high stability and a proper thermal match between the multilayer stack and the Tile Structure.

Each network utilizes 50Ω stripline waveguides buried into two substrate layers of the PTFE material RT6002 from Rogers [0.2]. The thickness of one RT6002 layer is about 0.50 mm and the dielectric constant is $\epsilon_r = 2.92$. The ground strips are designed above and below the centre line and are connected by a via chain on the left and right side of the centre line. Ground to ground vias through all three cores will connect the different ground levels within the EFN. Figure 4 illustrates the cross view of the multilayer board. A top and bottom CFRP panel are added for mechanical and thermal stabilisation of the multilayer network.

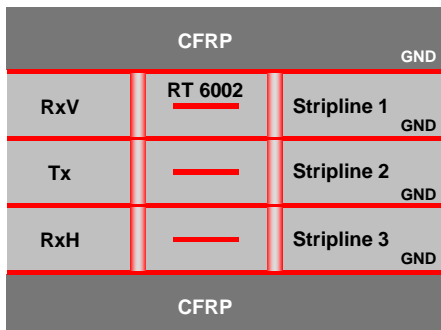


Fig. 4. Cross view of multilayer board

Wilkinson coupler, inter-layer transitions and transitions to GPO and SMA connectors have been designed and optimised using IMST's in-house software EMPIRETM,

which is based on the 3D Finite Differences Time Domain (FDTD) method. In the simulation the multi-layer stack with the substrate RT6002, the bonding films and prepregs was included. Buried waveguides have been designed in stripline technique with via chains to suppress the excitation of parallel plate modes between the covering ground planes. An other important issue was the proper modelling of the SMD resistors, which have been assembled into cavities of each Wilkinson divider. The electrical behaviour of this element was optimised with respect to return loss at all ports and isolation between the output ports. The following properties could be achieved for the specified frequency band: return losses > 30 dB and isolation of output ports > 35 dB.

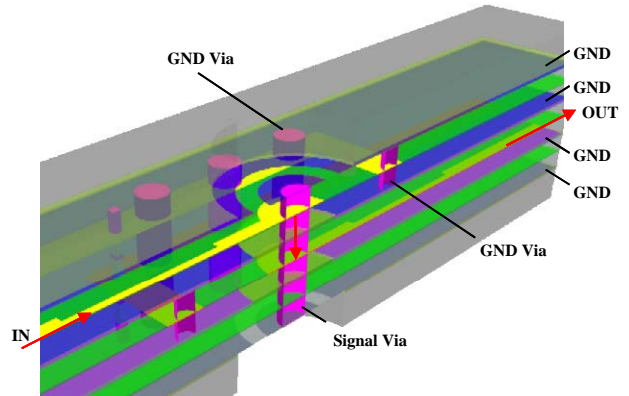


Fig. 5. 3D view into inter-layer transition

The circuit for the inter-layer transition needed for the two receive networks was designed with EMPIRE, too. Small matching circuits with steps in the centre line width were placed next to the transition to improve the electrical behaviour. The complete structure with all layers, the openings in the CFRP plates and the via holes is included in the simulation. This is illustrated in figure 5. The transition from the top triplate (IN) to the centre triplate waveguide (OUT) is presented in a cross section view. This kind of transition is required to route the signal lines from the top divider network to the centre divider network, where the input and output connectors are contacted. Signal and ground strips as well as signal and ground vias are visible in this transparent drawing. Simulations result into return losses better than 40 dB from DC up to 1.6 GHz.

3D FDTD optimisation was also necessary at the transitions from the buried stripline waveguides to the input and output connectors. At the seven output ports GPO connectors with right-angle plugs have been used. Five pins of the connector have been mounted through the substrates and soldered from the backside. The four outer pins are ground connections, while the centre pin is joined with the signal line of the stripline waveguide. The connector footprint is recessed into a top and bottom cavity of the multilayer substrate. Figure 6 illustrates this configuration in a cross view. Return loss is better than 35 dB up to 1.6 GHz.

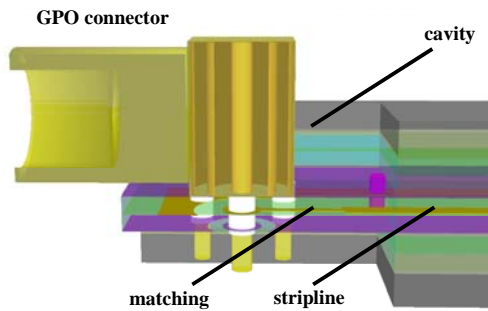


Fig. 6. 3D view into transition to GPO connector

At the three input ports 5-pins straight SMA connectors are utilized. The mounting technique is the same as described for the GPO connectors. Figure 7 illustrates the cross-section of this configuration. Optimisation does also result in a return loss better than 35 dB. For GPO and SMA connectors ideal coaxial waveguides have been assumed, since the real inner geometry and materials are not known. From the literature the return losses of these connectors are expected to be about 25 dB.

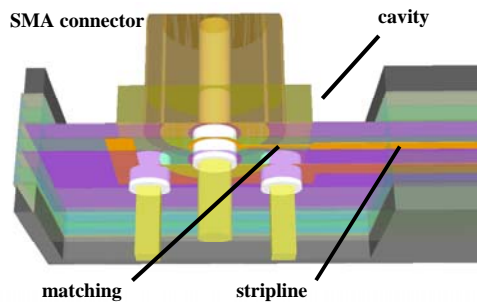


Fig. 7. 3D view into transition to SMA connector

The entire simulation and optimisation effort finally results into a multilayer Elevation Feed Network with a total size of about 120 cm x 20 cm x 0.6 cm. Radiation, susceptibility and thermal simulations (Fraunhofer IZM, Berlin) have been carried out, too. A couple of pre-development demonstrators have been manufactured at Cicorel in Switzerland, assembled and tested at IMST. Figure 8 shows a photo of Elevation Feed Network, while figure 9 gives an insight into the multilayer circuitry, generated from the 3D simulation tool editor Ganymede.



Fig. 8. Photograph of Elevation Feed Network

S-parameters measurements have been carried out at ambient conditions and in thermal cycling from -15 to

50°C. Moreover, EMC tests have been carried out: radiation measurements at IMST and susceptibility measurements at CRF, Italy. The first networks, which have been delivered to EADS-Astrium Portsmouth, GB, succeeded in further environmental characterisation and have been integrated into its satellite instrumentation to perform system tests. The development of the L-band Elevation Feed Network is funded by the European Space Agency ESA-ESTEC, Noordwijk [2.1]. Table 2 summarizes the properties of the module, obtained at ambient conditions.

Table 2. Characteristics of L-band divider networks

L-Band SAR Elevation Feed Network	
Centre Frequency	1.258 GHz
Bandwidth	70 MHz
Return Loss	> 25 dB
Insertion Loss (Tx)	< -11 dB
Transmission Loss	< -2 dB
Combiner Gain (Rx)	> 6dB
Amplitude Flatness	< 0.09 dB
Gain Balance	< 0.16 dB
Phase Balance	< 4°
Port Isolation	> 32 dB
Cross Talk	< -80 dB

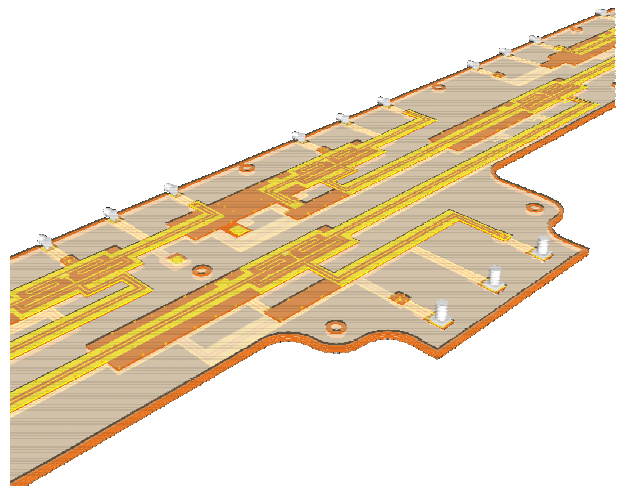


Fig. 9. Layout view of inner divider network structure

4. EASTON

The phased array antenna concept of the project HIFE [3.1] as part of an ESA ARTES-3 program, motivates the development of a power distribution network in multi-layer LTCC. Applications like satellite communication with broadband multimedia services are requiring solutions of that kind. The innovative antenna concept provides multiple beams with different directions of radiation. The main advantage is the flexible use of bandwidth exclusively in the desired ground zones.

A multiple beam concept implies that every antenna element has to receive the information of all participating beams. In order to maximize miniaturization, a compact distribution network was needed [3.4]. Within the EASTON project [3.3], funded by the German Space Agency, a power distribution module for Ka-band down-link (17-21 GHz) on multi-layer LTCC has been developed, which would fit into the concept of the HIFE project. LTCC has been chosen to stack two distribution networks (each with 1 input and 4 output ports) on top of each other within the multilayer ceramic. Each network consists of 3 Wilkinson dividers with buried screen printed resistors as well as several optimized waveguide transitions. Stripline technology has been utilized, while via chains suppress cross-talk from one part of the circuit to another. The final module demonstrates the benefits LTCC: compact size, low cost and reliable performance. Figure 1 shows a photo of the entire divider module.

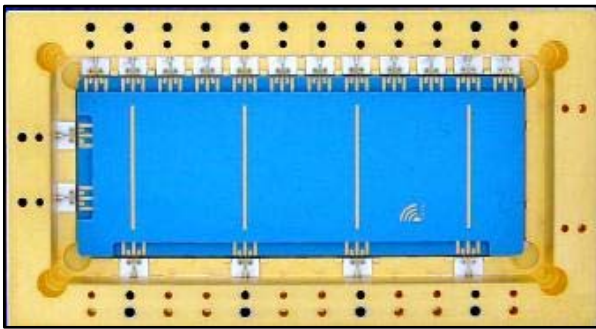


Fig. 10. Photo of divider module utilizing multilayer LTCC in a gold-plated DISPAL housing

The design and development activities within this project have been concentrated upon the optimisation of the buried stripline waveguides, the Wilkinson dividers with buried screen printed resistors [3.6] as well as the 5 different transitions within the multilayer LTCC and the housing [3.7]. Green Tape™ multilayer LTCC from DuPont has been selected [0.3] to develop the buried divider networks. Basic investigations have shown, that the multilayer ceramic is suitable to be used in microwave applications [0.4, 3.2, 3.5]. Figure 11 illustrates the layer setup: In total 10 layers with different tape thickness (A2 and AX) have been utilized to realise two buried striplines (SL₁ and SL₂) for the dividers and a microstrip line (MS) on top of the substrate. All RF-ports are on the same level at SL₁ at a height of 1mm. This requires interlayer transitions from MS to SL₁ and from SL₂ to SL₁. Further transitions are from the ports on the LTCC to the GPPO connectors within the DISPAL housing. Some selected results are described in the following sections.

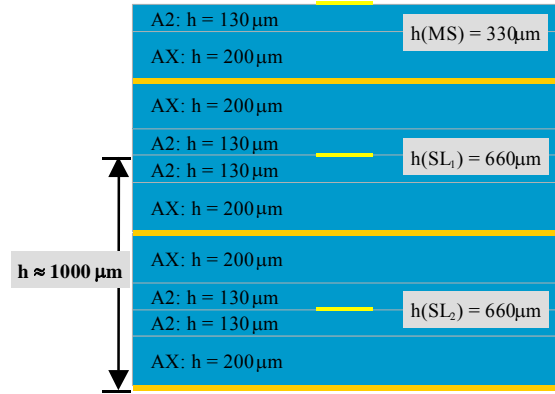


Fig. 11. Cross section of the divider module (material: Dupont 951, $\epsilon_r = 7.8$)

4.1 Wilkinson Dividers in LTCC

Each network includes one input and four output ports. A binary tree is formed of three Wilkinson dividers. The resistors thereof are buried components to provide short connections without additional parasitics. Wider strip lines give lower ohmic losses. Thus the inner line impedance of the strip lines was decided to be 30Ω . Therefore the resistor value of the Wilkinson divider is 60Ω . The optimisation of the divider design was done with the IMST in-house developed 3D FDTD field simulator EMPIRE™. Fig. 12 shows a Wilkinson divider in the software environment with visualised field distribution of the perpendicular electric field for two different field excitations. Via chains around the structure suppress unwanted cross-talk.

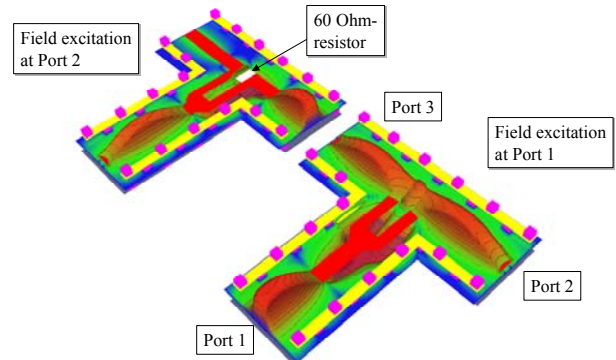


Fig. 12. Wilkinson divider in LTCC with electric field

In the next step three dividers were combined to a (1 : 4) distribution network. Optimum chamfered bends and interconnecting lines lead to an overall satisfying electrical behaviour. The structure together with the field distribution of the perpendicular electric field is shown in Fig. 13. The field excitation at port 2 gives a good imagination of the increasing isolation between adjacent output ports. The power is reduced by 3 dB at every divider stage. This relationship is illustrated nicely by the fading amplitude of the electric field.

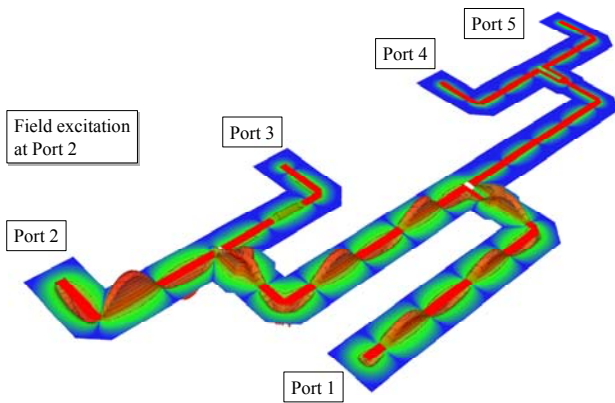


Fig. 13. (1 : 4) distribution network with electric field

4.2 Transitions and Connectors

Three different kinds of transitions have been designed and optimised for signal paths within the LTCC substrates and further two for the transition from the LTCC to the housing and the connectors [3.7], see figure 14:

- Microstrip $50\Omega \leftrightarrow$ Stripline \leftrightarrow Port in cavity 50Ω
- SL_1 $30\Omega \leftrightarrow$ Port in cavity 50Ω
- SL_2 $30\Omega \leftrightarrow$ Stripline \leftrightarrow Port in cavity 50Ω
- Ground-signal-ground wire-bonds:
Port in cavity \leftrightarrow Substrate in housing
- Substrate in housing \leftrightarrow GPPO connectors

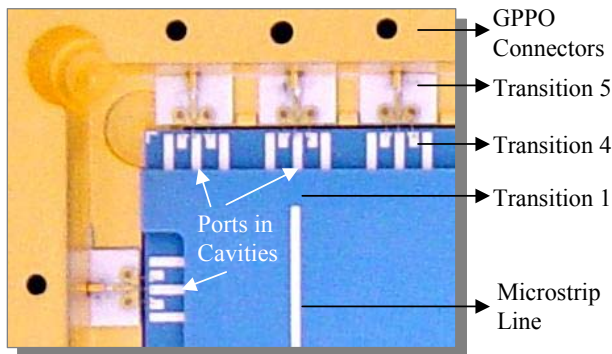


Fig. 14. Zoom of module's corner

One design task was to find a transition from the 50Ω microstrip line ($w = 390\mu\text{m}$) on top of the LTCC to the ground-signal-ground port in cavity. It becomes necessary to introduce a first step from micro-strip to stripline level followed by a via connection from stripline to microstrip configuration within the cavity of the port. As illustrated in Fig. 15 a complex routing of the ground conductors and vias has been preferred. This gives additional degree of freedom to optimise the transition's electrical performance. Furthermore ground strips and via chains improve the shielding of this part against other circuit branches. Cross-talk can be minimized this way.

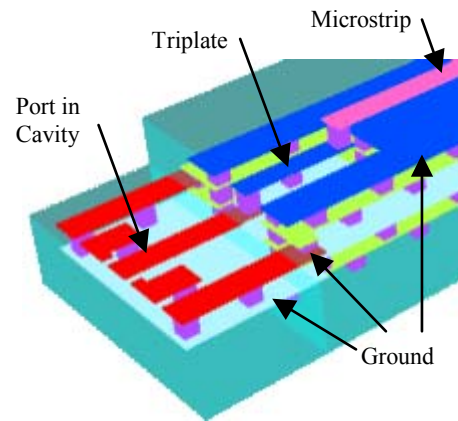


Fig. 15. Transition with shielding structures to minimize cross-talk: Microstrip \leftrightarrow Stripline \leftrightarrow Port in cavity

The final transition is even more complex. Two vertical steps from conductor level SL_2 to the port in cavity became necessary. An impedance transformation from 30Ω to 50Ω was also included. Figure 16 illustrates the cross-view of the centre line routing. Two steps with filled via connections have been introduced to pass the stripline waveguide to the port level. Again, transition and impedance transformation are guided by a top and bottom ground strip as well as a shielding via chain on the left and right hand side of the centre line. 3D simulations have shown, that this effort is mandatory to avoid cross-talk to neighbored branches. The success of the shielding configuration becomes evident, when the electrical field distribution in figure 16 is considered. Only low field concentrations can be found outside the ground cage. In the cavity on the left side of the graph the e-field is significant higher. Ground strips beside the ground-signal-ground pads of the port avoid coupling with adjacent ports (see figure 14).

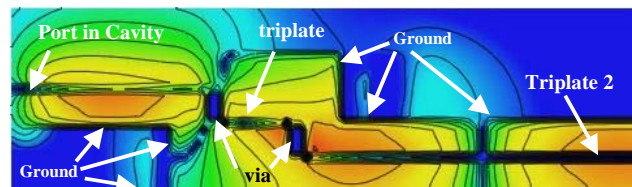


Fig. 16. Simulated electrical field in transition: Stripline SL_2 $30\Omega \leftrightarrow$ Stripline \leftrightarrow Port in cavity

All analysis has been made with the 3D Finite Differences Time Domain method. Project partners from the Technical University of Ilmenau have manufactured the LTCC tiles made of the DuPont tape 951. Silver and gold conductor paste systems have been utilized for two different modules. They have also optimised the buried screen printed resistors, which were necessary for the Wilkinson combiners [3.4] and [3.5]. TESAT Spacecom has designed and manufactured the DISPAL housing and has mounted and assembled the LTCC board into the package. The total size of the module is $6.5 \times 3.5\text{ cm}^2$. RF measurements have been performed at IMST in a frequency range up to 40 GHz. The measured

S-parameters agree very well with the simulated data. This has been published in [3.7] for all core transitions within the multilayer LTCC. With some further optimisations the specified return and insertion losses can be met in the desired frequency band from 17 to 21 GHz. Complex shielding effort has been made to minimize cross-talk among the divider and transmission line branches. As fundamental result of this R&D work it has been proven, that LTCC is a reliable substrate technology for space applications at GHz-frequencies.

5. ACKNOWLEDGEMENT

The author's wish to thank the German Space Agency (DLR) for funding and supporting the TerraSAR-X and EASTON activities. Sincere thanks are given to EADS-Astrium in Friedrichshafen, Germany, for many years of fruitful co-operation in TerraSAR-X. Faithful work has been carried out with the project partners from Technical University of Ilmenau and TESAT SPACECOM in EASTON. Particular acknowledge is given to EADS-Astrium in Portsmouth and ESA/ESTEC in Noordwijk for confidence in and supporting IMST's solution for TerraSAR-L.

6. SUMMARY

Although the three projects differ in details from each other, highly demanding solutions for single- and multi-layer power divider networks have been developed.

7. REFERENCES

0.1 E.J. Wilkinson, *An N-way Hybrid Power Divider*, IRE Transactions, MTT, Vol. MTT-13, pp. 116-118, January 1960.

0.2 Rogers Corporation, *RT/duroid™ 6002 PTFE Composite Circuit Board Material for Microwave Applications*, RT 1.600.

0.3 DuPont Green Tape™ Design and Layout Guideline

0.4 IMST's internet site about LTCC <http://www.ltcc.de>

7.1 References for TerraSAR-X

1.1 D. Köther, G. Pautz, G. Möllenbeck, P. Uhlig, W. Poppelreuter, A. Serwa, *1:30 Power Splitter with excellent Amplitude and Phase Accuracy over a wide Temperature Range*, Microaps Conference, Phoenix, 2001.

1.2 D. Köther, A. Lauer, A. Wien, P. Uhlig, G. Pautz, G. Möllenbeck, J. Berben: *X-Band 1:32 Divider Network for Space Application with Excellent Amplitude and Phase Balance*, EuMW 2003, Munich (Germany), 06.-10. October 2003.

1.3 D. Köther, A. Lauer, A. Wien, P. Uhlig, G. Pautz, G. Möllenbeck, J. Berben, *Reliable 1:32 Power Divider For Space Application*, Microwave Technology and Techniques Workshop, Preparing for Future Space Sys-

tems, Organised by the Microwave and Millimetre-Wave Section (TOS-ETM), ESA-ESTEC Noordwijk,, 11 – 12 May 2004.

1.4 D. Köther, *Advanced Techniques For The Production Of High Precision X-Band Power Distribution / Combination Networks*, 3rd European Microelectronics and Packaging Symposium EMPS 2004, Prague (Czech Republic), 16.-18. June 2004.

1.5 D. Köther, P. Uhlig, *Hochpräzise X-Band-Verteilnetzwerke für Erderkundungssatelliten*, Deutsche IMAPS-Konferenz 2004, München (Germany), 11.-12. October 2004.

7.2 References for TerraSAR-L

2.1 P. Vogel, M. Ludwig, K. van't Klooster, A. Head, *The L-Band SAR Pre-Development*, IGARSS: IEEE International Geoscience and Remote Sensing Symposium, Anchorage Alaska, 20-24 September 2004.

7.3 References for EASTON

3.1 J. Butz, M. Spinnler, J. Christ, U. Mahr, *Highly integrated RF-modules for Ka-band multiple-beam active phases array antennas*, IEEE MTT-S CDROM, pp. 61-64, Seattle, June 2002.

3.2 R. Kulke, W. Simon, C. Günner, G. Möllenbeck, D. Köther, M. Rittweger, *RF-Benchmark up to 40 GHz for various LTCC Low Loss Tapes*, IMAPS-Nordic, Stockholm, Proceedings pp. 97-102, 29. Sept.-2. Oct. 2002.

3.3 "EASTON" *Entwicklung eines Verteilernetzwerkes mit integrierter Antenne auf mehrlagigem LTCC Substrat*, FKZ: 50 YB 0007, German DLR Project, 2002.

3.4 R. Kulke, W. Simon, G. Möllenbeck, J. Kassner, P. Uhlig, S. Holzwarth, P. Waldow, *Power Distribution Networks in Multilayer LTCC for Microwave Applications*, Proceedings of the International Symposium on Microelectronics (IMAPS), pp. 321-324, Baltimore, October 2001.

3.5 R. Münnich, H. Thust, R. Kulke, *Multilayer LTCC-Module für HF-Anwendungen*, 10. Keramik-Tag der BAM, Symposium: *Folien- und Multilayer-technologie für funktionskeramische Anwendungen*; Berlin, Deutsche Keramische Gesellschaft e.V., 10. und 11. April 2003.

3.6 J. Kassner, R. Kulke, P. Uhlig, M., Rittweger, P. Waldow, R., Münnich, H. Thust, *Highly Integrated Power Distribution Networks on Multilayer LTCC for Ka-band Multiple-Beam Phased Array Antennas*, IMAPS Nordic Conference, Espoo, Finland, Proceedings pp. 51-54, 21.-24. September 2003.

3.7 R. Kulke, J. Kassner, G. Möllenbeck, M. Rittweger, P. Waldow, *Ka-Band Power-Distribution Networks on Multilayer LTCC for Broadband Satellite Multimedia Applications*, EuMC, Workshop WS-8: *Ceramic based Microwave Circuits*, Munich, Proceedings pp. 17-20, 6. October 2003.